



Brazilian Journal of Physics
ISSN: 0103-9733
luizno.bjp@gmail.com
Sociedade Brasileira de Física
Brasil

Alves, L. A.; Sagás, J. C.; Damião, A. J.; Fontana, L. C.
Drude's Model Optical Parameters and the Color of TiNx Films Obtained Through Reflectivity
Measurements
Brazilian Journal of Physics, vol. 45, núm. 1, 2015, pp. 59-63
Sociedade Brasileira de Física
São Paulo, Brasil

Available in: <http://www.redalyc.org/articulo.oa?id=46433753009>

- How to cite
- Complete issue
- More information about this article
- Journal's homepage in redalyc.org

redalyc.org

Scientific Information System
Network of Scientific Journals from Latin America, the Caribbean, Spain and Portugal
Non-profit academic project, developed under the open access initiative

Drude's Model Optical Parameters and the Color of TiN_x Films Obtained Through Reflectivity Measurements

L. A. Alves · J. C. Sagás · A. J. Damião · L. C. Fontana

Received: 3 September 2014 / Published online: 6 January 2015
© Sociedade Brasileira de Física 2014

Abstract Titanium nitride (TiN) has been applied as decorative coating due to its high reflectivity and goldish color, having high hardness and wear resistance. In the present work, TiN_x films were deposited by grid-assisted magnetron sputtering. The color and reflectivity were investigated by spectrophotometry as a function of the working gas ratio N_2/Ar used during films deposition. The crystalline phases were identified by X-ray diffraction pattern (XRD). The TiN_x plasma frequency (ω_p) and the relaxation time (τ) were determined by fitting the experimental reflectivity curves, according to the Drude model. The color parameters obtained by the Cielab method were used to compare TiN_x films with gold film.

Keywords Drude's model parameters · Sputtering · TiN films · Colorimetry

1 Introduction

Titanium nitride (TiN) is one of the most studied and used materials for hard coating applications. TiN films are chemically stable, corrosion resistant, and have high wear resistance [1–3]. An interesting characteristic of titanium nitride compounds (TiN_x) is the existence of metallic (Ti–Ti) and covalent

(Ti–N) bonding. Due to these characteristics, TiN_x presents metallic properties, such as electrical conductivity and metallic reflectance, and covalent bonding properties, such as high melting point, high hardness, and excellent thermal and chemical stability [1, 4]. Therefore, it is extensively used in a wide range of applications, from protective coating of machine parts and cutting tools, to applications as diffusion barriers in semiconductor technology and photocatalytic material [5, 6]. Moreover, TiN is used as a decorative coating due to its goldish color. However, in order to obtain a good tone matching between TiN_x and gold, it is important to make careful stoichiometric adjustments and to have the correct microstructure in the final coating material, by controlling the process deposition parameters [7, 8]. In magnetron sputtering processes, it is possible to control some parameters to tune the film properties [7, 9–11]. The film stoichiometry can be determined by the working gas flow ratio (N_2/Ar) during film deposition and, consequently, stoichiometry can also modify film reflectivity and color [12].

By using the Drude semi-classical model, it is possible to establish a correlation between the reflectivity and the density of free electrons in the film. This model assumes that the electrons from the valence band behave as a gas of electrons. Such electrons absorb the incident radiation energy and emit this energy as photons at a characteristic time, namely, the relaxation time (τ). This model is suitable for metals [13, 14], and it can also be applied for TiN_x [15–17] due to its metallic characteristics. This model allows us to establish a correlation between the electrical and the optical properties of the TiN_x films. From the Drude model, it is possible to demonstrate that the reflectivity (R) is given by [18, 19]:

$$R = \left| \frac{1 - \sqrt{\varepsilon_\infty - \frac{\omega_p^2 \tau}{(i - \omega \tau) \omega}}}{1 + \sqrt{\varepsilon_\infty - \frac{\omega_p^2 \tau}{(i - \omega \tau) \omega}}} \right|^2, \quad (1)$$

L. A. Alves · J. C. Sagás · L. C. Fontana (✉)
Universidade do Estado de Santa Catarina, UDESC, Plasma
Laboratory, Joinville, SC, Brazil
e-mail: luis.fontana@udesc.br

L. A. Alves
Centro Universitário Católica de Santa Catarina, Jaraguá do Sul, SC,
Brazil

A. J. Damião
Instituto de Estudos Avançados, IEAv, São José dos Campos, SP,
Brazil

where ω is the frequency of the incident radiation, ω_p is the plasma frequency, and ε_∞ is a constant related to inter-band transitions. The plasma frequency ω_p is defined in the Eq. 2:

$$\omega_p^2 = \frac{4\pi \cdot n \cdot e^2}{m_e}, \quad (2)$$

where n is the number density of electrons, e is the electric charge, and m_e is the effective mass of the electron [19].

This paper also investigates the color variations on CIELab 1976 space [20] of TiN_x films deposited with different working gas flow ratio (N_2/Ar), as the color depends on the TiN_x composition. TiN_x films were deposited onto brass commercial substrates covered with a 50- μm Cr-Ni thick layer. The films were deposited by grid-assisted magnetron sputtering at different working gas flow ratio N_2/Ar . The crystalline phases were identified through X-ray diffraction (XRD). From the reflectivity measurements as a function of wavelength, fitted by the Drude model, it was possible to determine the constants ω_p (plasma frequency) and τ (relaxation time) for each TiN_x film.

2 Experimental Methods

The films were deposited by a grid-assisted magnetron sputtering [21, 22] in a stainless steel chamber of 30 cm diameter \times 30 cm height. The base pressure was 2.0×10^{-6} Torr, produced by a system composed of a mechanical and a diffusion pump. In order to avoid contamination by oil vapor from the pumps, a cooled trap was placed between the vacuum system and the deposition chamber. Working gas flow (Ar and N_2 of 99.99 % purity) was controlled by two 20-sccm mass flow controllers. The power supply used for the plasma generation was a 120-Hz pulsed voltage (0–1000 V).

The reactive deposition of TiN_x was carried out by sputtering of Ti atoms from a titanium target (99.5 % purity) in a N_2/Ar plasma atmosphere at pressure of 2.5 mTorr, monitored by a capacitive pressure gauge. The substrate was a commercial metal alloy C360 brass covered with a Cr-Ni layer. Table 1 shows the deposition parameters. The deposition time (10 min) and grid-target distance (2.0 cm) were

Table 1 Deposition parameters of TiN_x films

Sample temperature (°C)	Target voltage (V)	I (A)	V_{bias} (V)	Pressure (mTorr)	Flow Ar (sccm)	Flow N_2 (sccm)	N_2/Ar
300 \pm 10	500	1.0	–50	2.5 \pm 0.1	2.32	2.00	0.86
				2.5 \pm 0.1	2.28	2.40	1.05
				2.5 \pm 0.1	2.28	2.80	1.23

The deposition time (10 min) and the grid-target distance (2.0 cm) were maintained constant

maintained constant. During the film deposition, negative DC bias (–50 V) was applied to the substrate in order to improve the crystalline structure and the adherence between film and substrate [23].

The crystalline phases of TiN_x films were identified by X-ray diffractometry (10–70°) using Cu- $\text{K}\alpha$ radiation. The color characterization was carried out through a commercial spectrophotometer (wavelength range 250–1000 nm) equipped with an integrating sphere. The thicknesses of TiN_x films were measured through their cross-sectional view by using scanning electron microscopy (SEM).

3 Results and Discussion

In order to compare gold to TiN_x reflectivity and colorimetry, measurements were taken from a gold film as well as from TiN_x films (both TiN_x and gold films were deposited onto commercial brass covered with a Cr-Ni thick layer of 50 μm ;

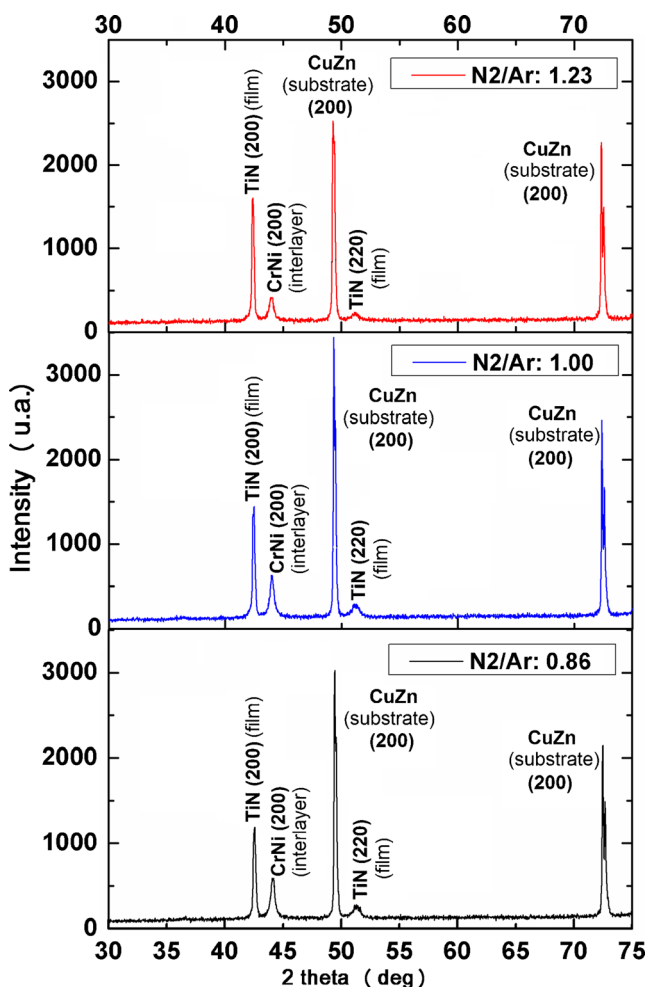


Fig. 1 XRD results of TiN films deposited for different working gas flow ratios N_2/Ar ; the peaks (200) (more intense) and (220) are observed. In the x-ray diffraction pattern, it is possible to see also peaks of brass substrate (CuZn) and peak of intermediate layer (Cr-Ni)

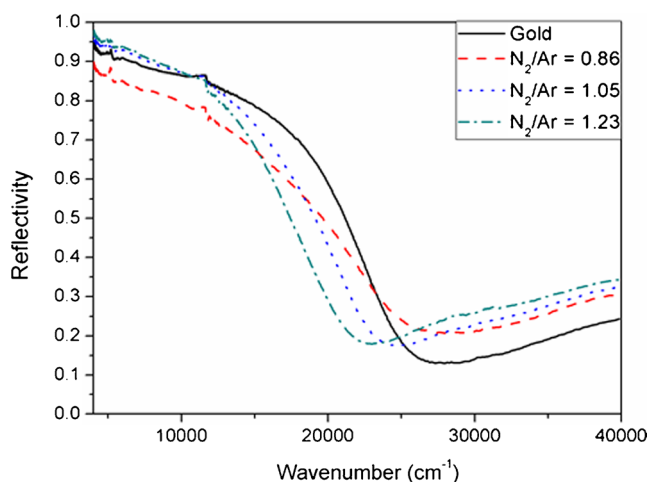


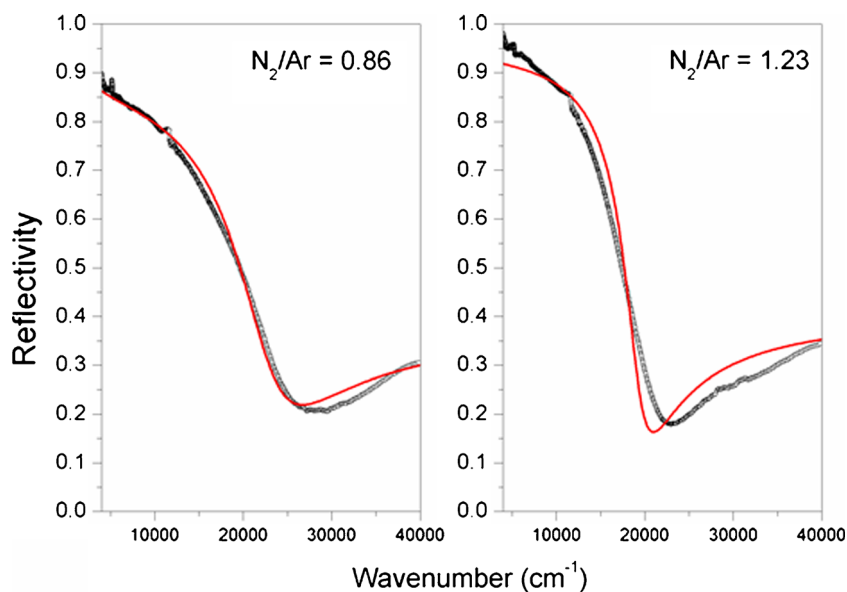
Fig. 2 Reflectivity as function of wavenumber for gold and TiN_x films

the gold film was deposited by electrochemical process while TiN_x was deposited by sputtering). An analysis of the reflectivity was made through the Drude model by fitting the experimental curve, allowing us to estimate the Drude equation coefficients.

3.1 XRD Results

The films obtained were visually yellow with nuances next to gold. Figure 1 shows the XRD results of TiN_x films deposited under different working gas flow ratio N_2/Ar . The TiN (200) phase peak was identified in the diffraction pattern, for all samples. To sum up, the results of this paper are in agreement with previous research which indicates that under similar deposition conditions, the most intense TiN peak is (200) [23]. In addition to TiN peak, it is also possible to observe substrate peaks in the XRD diffraction patterns (Fig. 1)

Fig. 3 Reflectivity curves obtained for two values of the N_2/Ar ratio 0.86 (left) and 1.23 (right). The points represent the experimental data and the fitting is the line



because the incident X-ray is diffracted in both, TiN_x films (thickness $1.0 \pm 0.2 \mu\text{m}$) and substrate.

3.2 Reflectivity

Figure 2 shows the reflectivity measurement of the TiN_x films compared to the gold one as a function of the wavenumber of incident radiation. The reflectivity curves of TiN_x films change as a function of N_2/Ar ratio and are similar to the gold reflectivity. It is possible to notice that for wavenumbers lower than $25,000 \text{ cm}^{-1}$ (corresponding to 400 nm wavelength), the TiN_x films' reflectivity is lower than gold, while for wavenumbers higher than $25,000 \text{ cm}^{-1}$, the reflectivity increases above the values of gold. This result shows that TiN_x films are more reflexive than gold in the violet and ultraviolet region.

Applying Eq. 1, it is possible to fit the reflectivity curves for each TiN_x film by adjusting the parameters ω_p (plasma frequency) and τ (relaxation time). These variables are related to the band structure of the material [17, 23]. The reflectivity curves show that it is possible to modify the response of reflectivity by a small change on the TiN_x film stoichiometry. It is related to the energy levels and density of charge carriers n in the material. Figure 3 shows the experimental reflectivity curves with the corresponding fit for N_2/Ar flow ratio of 0.86 and 1.23. The fitting was adjusted according to the Drude model using the free software RefFIT [24], which employs the Levenberg-Marquardt algorithm for non-linear fitting. The parameters ω_p (plasma frequency), τ (relaxation time), and the constant ϵ_∞ that were obtained from the fittings are listed in Table 2. It is observed that τ increases while ω_p decreases as the ratio N_2/Ar increases.

The plasma frequency is proportional to the electron density (see Eq. 2), while the relaxation time is associated with the

Table 2 Values of ε (related to inter-band transitions), ω_p (plasma frequency), and τ (relaxation time) obtained from the Drude model, by fitting the experimental curves

N_2/Ar	ε_∞	$\omega_p (\times 10^{15} \text{ s}^{-1})$	τ (fs)
0.86	17.3	2.93	3.70
1.05	19.4	2.83	7.14
1.23	20.2	2.63	9.10

semi-classical modeling of successive collisions among electrons in the valence band, i.e., the relaxation time is inversely proportional to the electron density [14, 19, 25]. Thus, the decrease in plasma frequency and the increase in relaxation time show a decrease in electron density with increased N_2/Ar flow ratio. A higher N_2/Ar flow ratio implies a higher amount of nitrogen to react with Ti and, consequently, the formation of a TiN_x film richer in nitrogen. The formation of Ti-N covalent bonds and consequent decrease of Ti-Ti metallic bonds lead to a reduction in electron density and the film becomes “more ceramic” with higher N_2/Ar flow ratio, which is reflected in the values of plasma frequency and relaxation time. This increased “ceramic character” of the higher N_2/Ar flow ratio film can also be observed in the fit accuracy: for higher values of N_2/Ar flow ratio, a poorer fit is obtained (Fig. 3b), as the Drude model is more suitable for metals.

3.3 Colorimetry

The colors can be quantified through the parameters defined by CieLab $L^*a^*b^*$ [20]. The Cartesian coordinates values L^* , a^* , and b^* provide a numerical representation of surface color, namely *brightness*, *green-red*, and *blue-yellow*, respectively.

The $L^*a^*b^*$ color coordinates for TiN_x films are showed in Table 3. It is possible to observe that the brightness L^* of gold is higher than TiN_x . Among samples covered with TiN_x , it was observed that the brightness L^* decreases as the N_2/Ar ratio increases. Given that the titanium nitride compounds (TiN_x) exhibit both metallic (Ti-Ti) and covalent (Ti-N) bonding, it can be expected (based on the decreased ω_p) that the proportion of covalent (Ti-N) increases with the increase in the N_2/Ar ratio. From the Drude model, n is the charge density of carriers and it is proportional to the reflectivity (associated with the brightness), thus increased N_2/Ar ratio results in decreased brightness.

For better viewing, we plot in Fig. 4 a comparison of color coordinates between gold and TiN_x films deposited with

Table 3 The $L^*a^*b^*$ color coordinates for different ratio N_2/Ar , compared to gold

	N_2/Ar	L^*	a^*	b^*
TiN_x	0.86	79.2	0.61	20.8
TiN_x	1.05	78.4	2.8	35.1
TiN_x	1.23	71.7	10.2	34.2
Gold	—	87.8	−0.53	28.1

different N_2/Ar ratio: panel a compares a^* and b^* and panel b shows L^* values. The a^* coordinate (associated with red tones) has large magnification as the N_2/Ar ratio increased. The smallest difference from gold is observed for TiN_x films deposited with lower N_2/Ar ratio ($N_2/Ar=0.86$). The b^* coordinate (associated with yellow tone) increases when the N_2/Ar ratio rises from 0.86 to 1.05 but, differently from a^* , it remains almost constant when the ratio increased from 1.05 to 1.23. This justifies the tone changes from yellow to red by increasing the N_2/Ar ratio. Figure 4b shows the L^* coordinate (associated with brightness), where a slight decrease is observed in L^* with increase in the N_2/Ar ratio, that is associated with decrease in charge density of carriers n , discussed above.

4 Conclusions

TiN_x films with preferred crystallographic orientation (texture) (200) deposited by grid-assisted magnetron

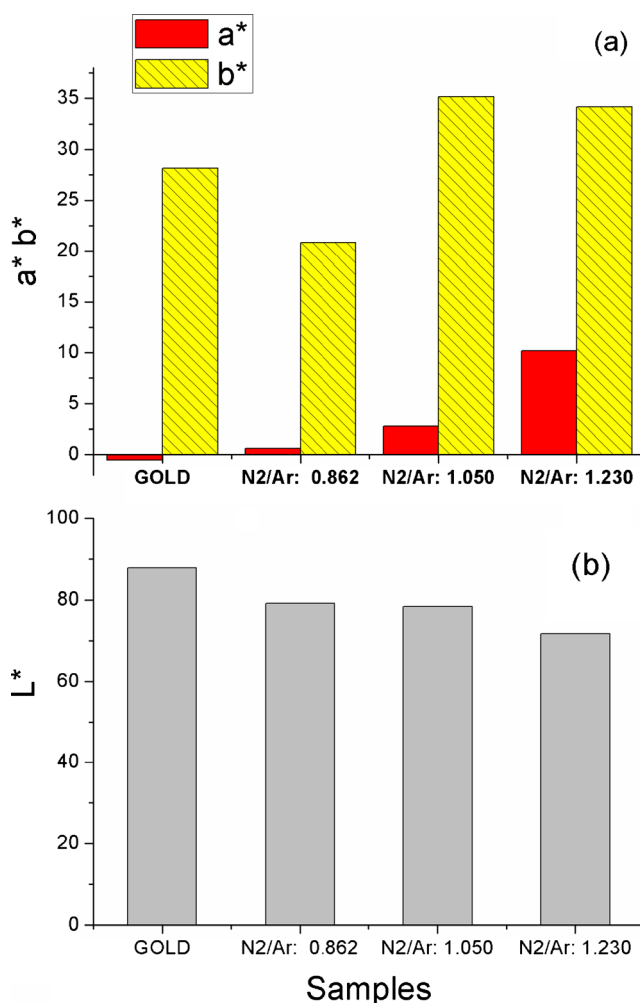


Fig. 4 Color coordinates of gold and TiN_x films deposited with different ratios N_2/Ar

sputtering show significant change in color from yellow golden to red tone, for a narrow range of N_2/Ar ratio in working gas during the film deposition ($0.8 < N_2/Ar < 1.2$). The spectrophotometry measurements showed that the color coordinates (CIE $L^* a^* b^*$) depend on the N_2/Ar ratio: the brightness (L^*) decreases slightly by increasing N_2/Ar while the chromaticity coordinate a^* increases continually and b^* coordinate reaches a plateau, giving higher red tones in TiN_x films when compared to gold. Applying the Drude model to fit the experimental reflectivity results, it is possible to estimate the values for ω_p (plasma frequency) and τ (relaxation time). It was observed that ω_p decreases while τ increases by increasing the ratio N_2/Ar . Based on the Drude model, the decrease in brightness (that is associated to the reflectivity) can be related to the decrease observed in plasma frequency (ω_p) and, therefore, related to reduction in charge carriers for higher concentration of nitrogen in TiN_x films.

Acknowledgments This project was sponsored by CAPES Brazil.

References

1. Y. Jyachandran, S. Narayandass, D. Mangalaraj, S. Areva, J. Mielczarski, Properties of titanium nitride films prepared by direct current magnetron sputtering. *Mater Sci Eng A* **445–446**, 223–236 (2007)
2. L.A. Rocha et al., Structural and corrosion behavior of stoichiometric and substoichiometric TiN thin films. *Surf Coat* **180–181**, 158–163 (2004)
3. Q. Luo, S. Yang, K.E. Cook, Hybrid hipims and DC magnetron sputtering of TiN coatings: deposition rate, structure and tribological properties. *Surf Coat Technol* **236**, 13–21 (2013)
4. T.-S. Yeh, W. Jenn-Ming, H. Long-Jang, The properties of TiN thin films deposited by pulsed direct current magnetron sputtering. *Thin Solid Films* **516**, 7294–7298 (2008)
5. A. Kumar, D. Kaur, Nanoindentation and corrosion studies of $TiN/NiTi$ thin films for biomedical applications. *Surf Coat Technol* **204**, 1132–1136 (2009)
6. M. Wittmer, H. Melchior, Applications of TiN thin films in silicon device technology. *Thin Solid Films* **93**, 397–405 (1982)
7. M. Nose, M. Zhou, E. Honboc, M. Yokotaa, S. Saji, Colorimetric properties of ZrN and TiN coatings prepared by DC reactive sputtering. *Surf Coat Technol* **142 a 144**, 211–217 (2001)
8. S. Niyomsoan, Variation of color in titanium and zirconium nitride decorative thin films. *Thin Solid Films* **415**, 187–194 (2002)
9. A. Lousa, J. Esteve, J. Mejia, A. Devia, Influence of deposition pressure on the structural mechanical and decorative properties of TiN thin films deposited by cathodic arc evaporation. *Vacuum* **81**, 1507–1510 (2007)
10. F. Vaz, P. Machado, L. Rebouta, J. Mendes, S. Lancer oz-Mendez, L. Cunha, S. Nascimento, P. Goudeau, J. Riviere, E. Alves, A. Sidor, Physical and morphological characterization of rectively magnetron sputtered TiN films. *Thin Solid Films* **420**, 421–428 (2002)
11. H. Durusoy, O. Duyar, A. Ayndilli, F. Ay, Influence of substrate temperature and bias voltage and the optical transmittance of TiN films. *Vacuum* **70**, 21–28 (2003)
12. G. Reiners, U. Beck, H. Jehn, Decorative optical coatings. *Thin Solids Films* **253**, 33–40 (1994)
13. A. Delin, Optical properties of the group-IVB refractory metal compounds. *Physical Review B* **54(3)**, 1673–1681 (1996)
14. B. Dominique e, T. Grosge, “Fitting the optical constantes of gold, silver, Chromium, titanium and adluminis in the visible bandwidht,” *Journal of Nanophotonics*, pp. 083097-1 - 083097-16, **07** (2014)
15. A. Perry, M. Georgson, W.D. Sproul, Variations in the reflectance of TiN , ZrN And HfN . *Thin Solid Films* **157**, 255–265 (1988)
16. P. Panjan, Optical properties of nitride coatings deposited at low substrate temperatures. *Vacuum* **40(1/2)**, 161–164 (1990)
17. B. karlsson, R.P. Shimshock, B.O. Seraphin, Optical properties of CVD-Coated TiN , ZrN and HfN . *Solar Energy Materials* **7**, 401–411 (1983)
18. A. Sadao, M. Takahashi, Optical properties of TiN films deposited by direct current reactive. *Journal of Applied Physics* **87(1)**, 1264–1269 (2000)
19. M.E.A. Kadi, Analysis of optical and related properties of thin oxide films determined by Drude-Lorentz model. *Surf Coat Technol* **211**, 45–49 (2012)
20. Gernot Hoffmann, “Cielab Color Space”, accessed april 1, 2012, <http://docs-hoffmann.de/cielab03022003.pdf>
21. L.C. Fontana, J.L.R. Muzart, Triode magnetron sputtering TiN film deposition. *Surf Coat Technol* **114(21)**, 7–12 (1999)
22. L.C. Fontana, J.L.R. Muzart, Characteristics of triode magnetron sputtering: the morphology of deposited titanium films. *Surf Coat Technol* **107**, 24–30 (1998)
23. J. Je, D. Noh, H. Kim, K. Liang, Preferred orientation of TiN films studied by a real time synchrotron x-ray scattering. *J Appl Phys* **81**, 6126 (1997)
24. A. Kuzmenko, *RefFIT - Software*, Geneva, accessed may 1, 2014, <http://optics.unige.ch/alexey/refffit.html> (2014)
25. M. Stromme, R. Karmhag, C. Ribbing, Optical constants of sputtered hafnium nitride films. Intra e interband contributions. *Opt Mater* **4**, 629–639 (1995)